WIDEBAND MIMO MEASUREMENTS OF OUTDOOR NLOS CHANNELS

Yaoqing Yang, Guanghan Xu, and Hao Ling
Department of Electrical and Computer Engineering
The University of Texas at Austin
Austin, TX 78712-1084

Received 2 August 2005

ABSTRACT: *The measurement results of the wideband wireless multiple-input multiple-output (MIMO) channels in outdoor environments are presented. Our wideband wireless MIMO channel sounder consists of four transmitters and eight receivers, and operates at a carrier frequency of 1.8 GHz with a bandwidth of 2.5 MHz. After obtaining the multipath delay profiles from the data collected in non-line-of-sight (NLOS) environments, realistic wideband MIMO channel capacities are computed and compared with the ideal channel simulation.* © 2005 Wiley Periodicals, Inc. Microwave Opt Technol Lett 48: 216–218, 2006; Published online in Wiley InterScience (www.interscience.wiley.com). DOI 10.1002/mop.21309

Key words: *wireless communication; wideband channel sounder; multipath delay profile; multiple-input-multiple-output channel capacity*

INTRODUCTION

Multiple-input multiple-output (MIMO) communication systems with multiple antennas at both the transmitter (TX) and the receiver (RX) ends have shown the potential of increased capacity in wireless channels. Realistic MIMO channels, however, usually contain some degree of spatial correlation among the multiple transmitting and receiving antennas. Consequently, the practical capacity may be lower than that expected from theoretical considerations [1]. During the past few years, researchers have used different ways to measure MIMO channel features. For example, a narrowband MIMO channel sounder with 16 transmitting antennas and 16 receiving antennas was employed to measure the channel characteristics in Manhattan [2]. A 2 TX by 2 RX wideband orthogonal frequency division multiplexing (OFDM) channel sounder was used to measure channel-impulse responses in suburban Chicago [3]. An 8 TX by 8 RX virtual wideband MIMO channel sounder that used fast switches at both the TX and RX ends was utilized to probe the indoor MIMO channels in picocell environments [4].

This paper presents the results of wideband wireless MIMO channel measurements with a true array channel sounder. Wideband MIMO channel measurement poses a challenge due to the high-data-acquisition requirement. Our system uses spread spectrum to simultaneously transmit multiple pseudo-random signals. Multiple receivers then receive the transmitted signals simultaneously. Such a system can most faithfully capture the wideband MIMO channel features in a real environment. A series of field measurements under non-line-of-sight (NLOS) scenarios is conducted at the J. J. Pickle Research Campus, the University of Texas at Austin. From the raw channel data, power delay profiles are extracted based on the cross-correlation property between the transmitted and received signals. MIMO channel capacities are then calculated from the measured channel data and compared with the independent, identically distributed (iid) channel simulation.

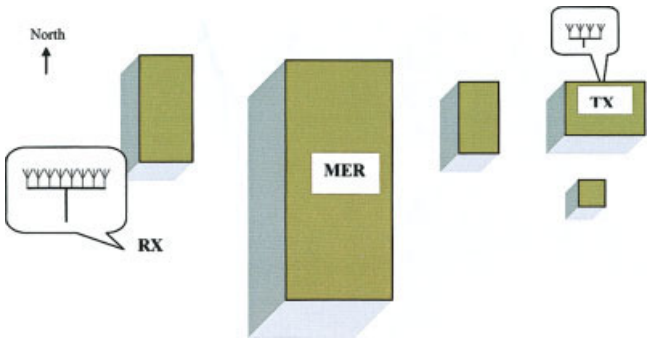

Figure 1 Top view of the NLOS measurement environment. [Color figure can be viewed in the online issue, which is available at www.interscience.wiley.com.]

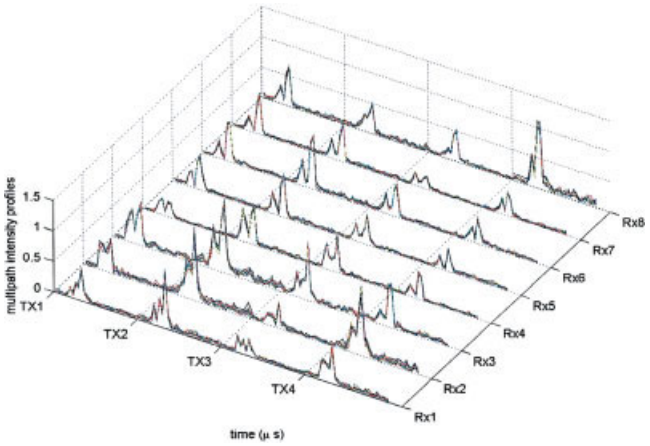

Figure 2 Sample power delay profiles of the 4 × 8 wideband MIMO channel. [Color figure can be viewed in the online issue, which is available at www.interscience.wiley.com.]

MEASUREMENT SETUP

Our wideband channel sounder consists of four transmitters and eight receivers that operate at a carrier frequency of 1.8 GHz. Each transmitter transmits the shifted version of a pseudo-random signal with a bandwidth of 2.5 MHz. The data length of a period of the TX sequence is 752. The four TX data sequences are simultaneously converted into analog baseband signals via four digital-to-analog converters and a field-programmable grid array. They are then mixed with an intermediate frequency (IF) local oscillator signal, and upconverted into radio frequency (RF) signals at 1.8 GHz. In the RX testbed, the RF signals are first down-converted to IF signals at 138.625 MHz, and then demodulated into baseband signals. Eight pairs of in-phase and quadrature-phase baseband signals are sent to four National Instruments data acquisition cards (PCI-6115). The sampling rate of the analog-to-digital converter is 10 MHz. The baseband signals are digitalized at 12-bit resolution. The collected channel data are stored onto a computer for post-processing. The maximum excess delay that can be measured by our system is 12 μs. The minimum delay that can be resolved is 0.4 μs. Therefore, the MIMO channel sounder is well suited for channel measurements in outdoor microcell scenarios.

An experiment campaign is conducted within the J. J. Pickle Research Campus, the University of Texas at Austin. Figure 1 shows the top view of the measurement environment. There are no tall buildings or physical structures nearby. On the roof of the building to the east, the transmit testbed and the TX antenna array are fixed. The RX antenna array is located to the west of the large MER building, which is about 25 m in height and blocks the direct path between the TX and RX. The distance between the TX and the RX is approximately 220 m. On the southern side, a row of

buildings contributes to reflective radio paths (not shown in the figure). The TX is a four-element linear array with a fixed element spacing of 1λ, where λ is the radio wavelength. The array elements are quarter-wave monopoles. The height of the TX antenna array is about 6 m above the ground. The RX is an eight-element linear array. The array elements are co-linear dipoles. The RX antenna array stands 0.6 m above the ground. Data are collected for two different element separations in the RX array, 1λ and 0.5λ.

EXPERIMENTAL RESULTS

Figure 2 shows the 4 × 8 multipath delay profiles or multipath intensity profiles (MIP) of the MIMO channel from the NLOS environment. The RX antenna elements are spaced 0.5λ apart. Four delay profiles are staggered along each time axis in order to show the profiles corresponding to the four transmitters. One snapshot of measurement captures 10,000 data samples from each RX antenna, which amounts to 12 periods of the transmitted sequence. Based on each period of data, we calculate the channel impulse response by using cross-correlation between the RX data and the TX sequences. Figure 2 actually shows all 12 periods of the multipath delay profiles superimposed on top of each other. The curves overlap and are nearly indistinguishable. Thus the channel is quite stable within a snapshot. It is also observed that two or three resolvable multipaths exist for each subprofile.

In order to evaluate the small-scale fading characteristics of the MIMO channel, measurements are taken according to the RX array location. Three snapshots per RX location are taken as the RX array is shifted by a short distance of 0.1λ. Therefore, 3600 channel samples are gathered over a distance of 10λ. After obtaining the channel-impulse responses over the locations of interest, we evaluate the channel capacity. The capacity of a wideband MIMO channel has been calculated by dividing the frequency band of interest into Ω narrowband frequency bins, each having a bandwidth of 1/Ω Hz [5]. The wideband MIMO channel capacity C_{wb} can be expressed as a summation of the narrowband capacities as follows:

$$C_{wb} = \frac{1}{\Omega}\sum_{f=1}^{\Omega} \log_2\left[\det\left(\mathbf{I}_N + \frac{\rho}{M}\mathbf{H}(f)\mathbf{H}(f)^H\right)\right], \qquad (1)$$

where $\mathbf{H} \in C^{M\times N}$ is the channel transfer function with M TX antennas and N RX antennas, ρ represents the average signal-to-noise ratio, and $(\bullet)^H$ denotes the Hermitian transpose of a matrix. Since the actual received signal strength varies with the TX and RX locations, a channel normalization is necessary to facilitate a comparison of the capacities at different locations. One reasonable normalization is to scale the channel matrix such that the average power transfer between a TX and an RX antenna is unity [6]. Therefore, the Frobenius norm is applied to normalize $\mathbf{H}(f)$:

$$\hat{\mathbf{H}}(f) = \mathbf{H}(f) \times \left[\frac{1}{\Omega MN}\sum_{f=1}^{\Omega} \|\mathbf{H}(f)\|_F^2\right]^{-1/2} \qquad (2)$$

and $\hat{\mathbf{H}}(f)$ is used in place of $\mathbf{H}(f)$ in Eq. (1).

Based on the measured data and an assumed signal-to-noise ratio of ρ = 20 dB, the wideband MIMO channel capacities versus RX locations are shown in Figure 3(a). The capacity is averaged over 36 channel samples at each RX location. We note that while the channel capacities from the measured data fluctuate along the RX locations, the capacity with an RX element spacing of 1λ is almost always higher than that with an RX element spacing of 0.5λ. This result is reasonable, since the increase in antenna element spacing causes the

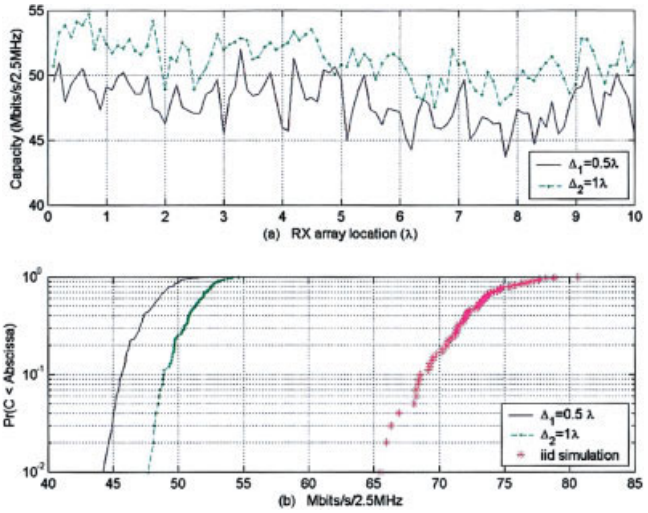

Figure 3 Wideband MIMO channel capacity: (a) capacity vs. receiver location for two different RX antenna element spacings; (b) outage probability of the channel capacity from the measured data and the iid assumption. [Color figure can be viewed in the online issue, which is available at www.interscience.wiley.com.]

MIMO channels to become less correlated. Consequently, a higher capacity can be achieved. Figure 3(b) shows the outage probability of the wideband MIMO capacity with the same signal-to-noise ratio of 20 dB. It is observed that the channel capacities from the measured data are significantly less than that based on the iid channel assumption. At the 10% outage probability, the wideband MIMO channel capacities obtained from the measured data are 46 and 48.5 Mbs/s with an RX element spacing of $\Delta_1 = 0.5\lambda$ and $\Delta_2 = 1\lambda$, respectively. By doubling the RX element spacing, the capacity increases by around 5%. However, at the same outage probability, the ideal capacity based on the iid channel assumption is 68 Mbs/s. Therefore, the capacity from the actual measured NLOS channels is achieved by about 70% of the ideal capacity.

CONCLUSION

We have presented the measurement results of wideband MIMO channels in an outdoor environment using a true array channel sounder. Our sounder consists of four transmitters and eight receivers with 2.5 MHz of bandwidth, and is capable of capturing all 32 channels of data simultaneously. After obtaining the multipath delay profiles from the data collected in an NLOS environment, the wideband MIMO channel capacities were computed and found to be about 70% of the ideal channel simulation.

ACKNOWLEDGMENTS

This work is supported by Texas Higher Education Coordinating Board under the Texas Advanced Technology Program, a research grant from The University of Texas at Austin, and the National Science Foundation Major Research Instrumentation Program.

REFERENCES

1. D. Shiu, G.J. Foschini, M.J. Gans, and J.M. Kahn, Fading correlation and its effects on the capacity of multielement antenna systems, IEEE Trans Commun 48 (2000), 502–513.
2. J. Ling, D. Chizhik, P. Wolniansky, R. Valenzuela, N. Costa, and K. Huber, Multiple transmit multiple receive (MTMR) capacity survey in Manhattan, Electron Lett 37 (2001), 1041–1042.
3. M.D. Batariere, T.K. Blankenship, J.F. Kepler, T.P. Krauss, I. Lisica, S. Mukthavaram, J.W. Porter, T.A. Thomas, and F.W. Vook, An experi-

mental OFDM system for broadband mobile communications, IEEE Vehic Technol Conf 4 (2001), 1947–1951.
4. B.T. Maharaj, J.W. Wallace, L.P. Linde, and M.A. Jensen, Frequency scaling of spatial correlation from co-located 2.4 and 5.2 GHz wideband indoor MIMO channel measurements, Electron Lett 41 (2005), 65–66.
5. D.P. Palomar, J.R. Fonollosa, and M.A. Lagunas, Capacity results of spatially correlated frequency-selective MIMO channels in UMTS, IEEE Vehic Technol Conf 2 (2001), 553–557.
6. J.W. Wallace, M.A. Jensen, A.L. Swindlehurst, and B.D. Jeefs, Experimental characterization of the MIMO wireless channel: Data acquisition and analysis, IEEE Trans Wireless Commun 2 (2003), 335–343.

EXPERIMENTAL STUDY OF ULTRA-BROADBAND PATCH ANTENNA USING A WEDGE-SHAPED AIR SUBSTRATE

Feng-Wei Yao, Shun-Shi Zhong, and Xian-Ling Liang
School of Communication and Information Engineering
Shanghai University
Shanghai 200072, P. R. China

Received 30 July 2005

ABSTRACT: *In this paper, an ultra-broadband patch antenna using a wedge-shaped air dielectric substrate is introduced. By adjusting the angle α, the experimental ratio bandwidth of $S_{11} \leqslant -10$ dB reaches 8.8:1, covering frequencies from 3.05 to 26.87 GHz. The measured impedance locus and radiation patterns at $f = 6$ GHz and at $f = 18$ GHz both are presented, and they show broadband characteristics and stability across the whole operating frequency bands, respectively.* © 2005 Wiley Periodicals, Inc. Microwave Opt Technol Lett 48: 218–220, 2006; Published online in Wiley InterScience (www.interscience.wiley.com). DOI 10.1002/mop.21310

Key words: *patch antenna; ultra-broadband; wedge-shaped; air substrate*

1. INTRODUCTION

Modern trends in wireless communication systems require ultra-wide-bandwidth antennas, by which the voice, data, and video information can be transmitted. Some of these wireless-communication system applications include fixed broadband local multipoint communication services, small mobile units such as cellular phones or other handheld units, laptops, and various remote-sensing devices. Most of these applications also require miniaturized antennas.

To enhance the microstrip antenna's operating bandwidth, a simple solution is to use thicker dielectric substrates. However, since a thick substrate is economically undesirable, variously shaped substrates have been proposed, such as stepped dielectric microstrip antennas and wedge-shaped microstrip antennas [1]. Also, low-permittivity materials such as air have been utilized as dielectric substrates in order to improve the bandwidth, as described below. It has been shown that the bandwidth of a U-slot microstrip antenna and an E-shaped patch antenna can reach 30% to 40% [2, 3]. An operational bandwidth of 95% for a 3D microstrip antenna has been investigated [4]. Moreover, a broadband patch antenna with a W-shaped ground plane has been proposed [5].

In this paper, we present an ultra-broadband patch antenna using a wedge-shaped air dielectric substrate, which contains three bandwidth improving elements: "wedge shape," "air dielectric substrate," and "leaflike patch." The experimental results demonstrate not only the bandwidth improvement, but also realization of miniaturization. Its structure and experimental results are presented as follows.

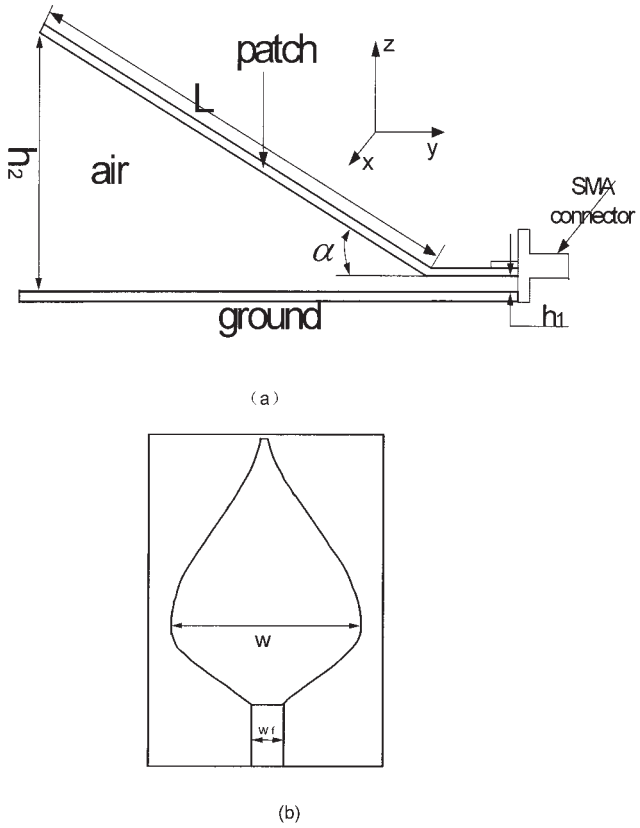

Figure 1 Structure and design parameters of the antenna: (a) side view; (b) top view

2. ANTENNA DESIGN

The proposed antenna consists of a leaflike patch and a ground plane, with a wedge-shaped air substrate between them, as shown in Figure 1. The leaflike patch with dimensions $w \times L$ is in a shape of a cosine-square taper. The minimal and maximum distances between the patch and ground are h_1 and h_2, respectively, with $h_1 = 1$ mm and h_2 being about a half-wavelength of the low-end operating frequency. An angle α between the patch and ground

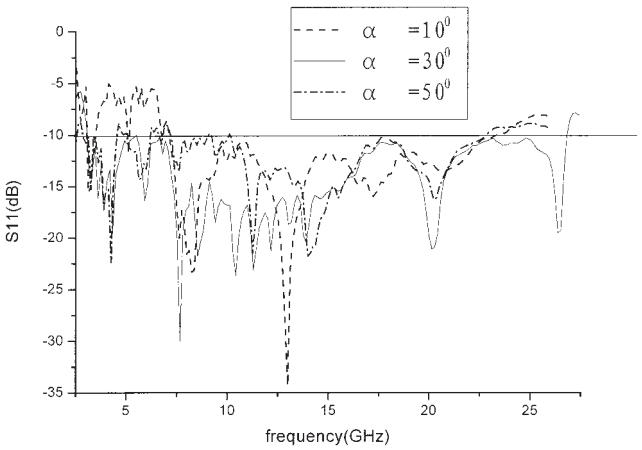

Figure 2 Measured return loss at various angles